

# Photocontrolled microphase separation in a nematic liquid–crystalline diblock copolymer

Haifeng Yu <sup>a,b,\*</sup>, Takaomi Kobayashi <sup>b</sup>, Guo-Hua Hu <sup>c</sup>

<sup>a</sup> Top Runner Incubation Center for Academia-Industry Fusion, Nagaoka University of Technology, 1603-1 Kamitomioka, Nagaoka 940-2188, Japan

<sup>b</sup> Department of Materials Science and Technology, Nagaoka University of Technology, 1603-1 Kamitomioka, Nagaoka, Niigata 940-2188, Japan

<sup>c</sup> Laboratory Reactions and Process Engineering, Nancy University, CNRS-ENSIC-INPL, 1 rue Grandville, BP 20451, 54001 Nancy, France

## ARTICLE INFO

### Article history:

Received 26 October 2010

Received in revised form

25 January 2011

Accepted 29 January 2011

Available online 24 February 2011

### Keywords:

Liquid–crystalline diblock copolymer

Microphase separation

Supramolecular cooperative motion

## ABSTRACT

Using a bromo-terminated poly(ethylene oxide) as a macroinitiator, an amphiphilic liquid–crystalline (LC) diblock copolymer with an azobenzene moiety as a nematic mesogen was prepared by an atom transfer radical polymerization process. In thin films of the well-defined diblock copolymer with the mesogenic block as a continuous phase upon microphase separation, the influence of supramolecular cooperative motion on the microphase-separated nanocylinders was systematically studied. Although the major phase of the hydrophobic nematic LC block showed only one-dimensional order, it could endow the separated minor phase of the hydrophilic PEO nanocylinders with three-dimensionally ordered structures. Both out-of-plane perpendicular and in-plane parallel patternings of the regularly ordered nanocylinder arrays were successfully fabricated on macroscopic scales by thermal annealing and photoalignment, respectively. The microphase-separated nanostructures with high regularity showed excellent reproducibility and mass production, which might guarantee nanotemplated fabrication processes and would lead to novel industrial applications in macromolecular engineering.

© 2011 Elsevier Ltd. All rights reserved.

## 1. Introduction

Liquid crystals (LCs) and block copolymers (BCs) are two kinds of soft materials with self-organizing nature, which are elegantly combined in one organic system of liquid–crystalline block copolymers (LCBCs). On the one hand, LCBCs inherit LC performances such as self-assembly, long-range ordered fluidity, molecular cooperative motion, formed large birefringence, anisotropy in various physical properties (optical, electrical and magnetic fields), and alignment change by external fields at surfaces and interfaces [1,2]. On the other hand, they can microphase separate into varieties of nanostructures like spheres, cylinders, lamellae phase domains with an increase in volume ratio of the LC block [3–9]. In thin films of LCBCs, the interplay function between the microphase separation and the elastic deformation of LC ordering, known as supramolecular cooperative motion (SMCM) [10–12], plays an important role in formation of hierarchical structures, which enables their microphase-separated nanostructures to be

manipulated into an ordered array along with the alignment direction of the mesogenic block.

According to SMCM, we systematically studied the microphase-segregated behaviors of a series of novel amphiphilic smectic LCBCs consisting of flexible poly(ethylene oxide) (PEO) as a hydrophilic segment and polymethacrylate containing an azobenzene (AZ) moiety in side chain as a hydrophobic LC block [10–15]. Upon microphase separation, the PEO-based LCBCs showed regular patternings of the PEO nanocylinder array as the minor phase, periodically dispersed in the AZ LC matrix. A vertically orientated pattern of PEO nanocylinders was obtained upon annealing with the help of out-of-plane alignment of AZ mesogens showing a smectic LC phase [10–17]. Whereas a homogeneously orientated pattern of PEO nanocylinders was fabricated by the in-plane homogeneous alignment of AZ mesogens induced either by a rubbing technique or a polarized laser beam [10–12]. It was believed that the layer structure of the smectic LC block might be one of the key factors to fabricate the homeotropic and homogeneous alignment of PEO nanocylinder arrays on macroscopic scales [10–12]. The SMCM exerts a great effect on LCBCs and enables the phase-segregated nanostructures to be arranged in an alignment direction perpendicular to the layers of the smectic LC with two-dimensional (2D) order. However, the influence of SMCM on the

\* Corresponding author. Department of Materials Science and Technology, Nagaoka University of Technology, 1603-1 Kamitomioka, Nagaoka, Niigata 940-2188, Japan.

E-mail address: [yuhafeng@mst.nagaokaut.ac.jp](mailto:yuhafeng@mst.nagaokaut.ac.jp) (H. Yu).

microphase separation of LCBCs possessing a nematic LC phase with one-dimensional (1D) order still remains unclear.

In this paper, we report on the microphase-separated behaviors in thin films of a PEO-based amphiphilic LCBC with AZ moieties as nematic mesogens under the influence of SMCM. Although a nematic LC shows lower ordering than a smectic one, it often has a lower viscosity than the latter. Moreover, AZ-containing nematic LC polymers have been extensively studied as photonic materials because of their quick response to light [2, 18–22]. It is expected that microphase-separated nanostructures can also be supramolecularly assembled in the designed nematic LCBC with well-defined structures and the formed phase-segregated nanostructures can be quickly manipulated by polarized light due to the existence of photoresponsive AZs as nematic mesogens.

## 2. Experimental section

### 2.1. Materials

2-Bromo-2-methylpropionyl chloride, triethylamine, phenol, 6-chloro-1-hexanol, methacryloyl chloride, *N,N*-dimethylformamide (DMF), 4-ethoxyaniline, hydroquinone, sodium nitrite, potassium carbonate and hydrochloric acid were commercially available (Kanto Chem. Co.) and used without further purification. Poly(ethylene glycol) monomethyl ether with a number-averaged molecular weight of about 5000 g/mol (Aldrich) was dried by azeotropic distillation with toluene. Anisole and tetrahydrofuran (THF) were purified by distillation from sodium with benzophenone. The ligand, 1,1,4,7,10,10-hexamethyltriethylenetetramine (HMTETA, Aldrich) was used as received without further purification. Catalyst copper (I) chloride (Cu(I)Cl) was washed successively with acetic acid and ether, then dried.

#### 2.1.1. 4-Ethoxy-4'-hydroxyazobenzene

4-Ethoxyaniline (20 g, 0.146 mol) was dissolved in a solution of hydrochloric acid (280 mL, 2 M) and the resulting solution was cooled at 0 °C. Sodium nitrite (10.1 g, 0.146 mol) dissolved in water (200 mL) was added dropwise into the solution to produce diazonium salt. A mixture of phenol (13.7 g, 0.146 mol) and sodium hydroxide (17.5 g, 0.438 mol) dissolved in water (250 mL) was added slowly at 0 °C, and then a yellow solid precipitated. The reaction mixture was stirred at room temperature for 2 h. After hydrochloric acid (2 M) was added to the reaction mixture to give pH = 3, the precipitated solid was collected and extracted with chloroform. The chloroform layer was dried with magnesium sulfate. After the solvent was removed, the crude product was purified by column chromatography on silica gel (ethyl acetate: *n*-hexane = 3:1) and then recrystallization from ethanol to obtain the purified product (22.5 g, 0.092 mol) in 64% yield. <sup>1</sup>H NMR (CDCl<sub>3</sub>, 300 MHz): δ 1.5 (t, 3H), 4.1 (q, 2H), 5.4 (s, 1H), 7.0 (m, 4H), 7.9 (m, 4H).

#### 2.1.2. 4-Ethoxy-4'-(6-hydroxyhexyloxy) azobenzene

A mixture of 4-ethoxy-4'-hydroxyazobenzene (11.0 g, 45 mmol) and 6-chloro-1-hexanol (9.3 g, 68 mmol) was dissolved in DMF (200 mL), and potassium carbonate (9.3 g, 68 mmol) was added to the solution. The resulting solution was refluxed for 12 h. After the reaction mixture was cooled to room temperature, the product was precipitated in water and then extracted with chloroform. The chloroform layer was dried with magnesium sulfate. After the solvent was removed, the crude product was purified by recrystallization from methanol to obtain product (13.5 g, 0.039 mol) in 87% yield. <sup>1</sup>H NMR (CDCl<sub>3</sub>, 300 MHz): δ 1.2–1.9 (m, 11H), 3.7 (t, 2H), 4.1 (m, 4H), 7.0 (m, 4H), 7.9 (m, 4H).

#### 2.1.3. 6-(4-(4-Ethoxyphenylazo)phenoxy)-hexyl methacrylate (M6ABOC2)

4-Ethoxy-4'-(6-hydroxyhexyloxy) azobenzene (1.5 g, 4.3 mmol) and triethylamine (0.26 g, 4.5 mmol) were dissolved in THF (30 mL) at 0 °C in an ice bath. Then a solution of methacryloyl chloride (0.23 g, 4.5 mmol) in THF (10 mL) was added dropwise under the protection of N<sub>2</sub>. The reaction mixture was stirred overnight. 100 mL deionized water was added, and the product was extracted with chloroform. After purification by column chromatography on silica gel (chloroform) and then recrystallization from methanol to obtain the purified product (1.4 g, 3.4 mmol) in 80% yield. <sup>1</sup>H NMR (δ, CDCl<sub>3</sub>, 300 MHz): 1.17 (t, 3H), 1.36–1.42 (m, 4H), 1.64 (t, 2H), 1.74 (t, 2H), 1.88 (s, 3H), 3.97 (q, 2H), 4.03–4.12 (m, 4H), 5.48 (d, 1H), 6.04 (d, 1H), 6.92 (m, 4H), 7.78 (m, 4H). λ<sub>max</sub> (chloroform) = 360 nm.

### 2.2. Synthesis of the macroinitiator PEO-Br

The macroinitiator was prepared by a Schotten–Baumann reaction between 2-bromo-2-methylpropionyl chloride and poly(ethylene glycol) monomethyl ether in dichloromethane (CH<sub>2</sub>Cl<sub>2</sub>) with a yield of about 32% (12). The molecular weight (GPC, relative to PS standards), polydispersity index and the melting temperature were 7400 g/mol, 1.02, and 64 °C, respectively.

### 2.3. Nematic LCBC (PEO-*b*-PM6ABOC2)

Cu(I)Cl (7.43 mg, 0.075 mmol), PEO-Br (125 mg, 0.025 mmol) and M6ABOC2 (923 mg, 2.25 mmol) were mixed in a 20 mL ampoule, degassed and filled with argon. HMTETA (20.4 μL, 0.075 mmol) in anisole (5.0 mL) was added. The mixture was degassed by three freeze-pump-thaw cycles and sealed under vacuum, and placed in an oil bath preheated at 80 °C for 24 h. Then the solution was passed through a neutral Al<sub>2</sub>O<sub>3</sub> column to remove the catalyst. The filtrate was precipitated into methanol. The copolymer was collected and dried. Yield: 742 mg (71%). Mn (GPC) = 31, 200, Mw/Mn = 1.17. The LCBC showed good solubility in organic solvents, such as THF, chloroform, toluene, DMSO, DMF and anisole.

### 2.4. Characterization

<sup>1</sup>H NMR spectra were measured using a Lambda-300 spectrometer operating at 300 MHz with tetramethylsilane as an internal reference for chemical shifts. The molecular weights of polymers were determined by gel permeation chromatography (GPC, JASCO) with standard polystyrenes in chloroform as eluent. The thermal properties of the monomers and polymers were analyzed by a differential scanning calorimeter (DSC, Seiko) at a heating and cooling rate of 10 °C/min. At least three scans were performed to check the reproducibility. The LC phases were evaluated with a polarizing optical microscope (POM, Olympus BH-2) equipped with a hot stage. The UV–vis absorption spectra were measured using a JASCO V-550 spectrophotometer.

### 2.5. Film preparation and photoalignment of LCs

The diblock copolymer films with a thickness of about 100 nm were prepared by spin-coating its toluene solution on clean glass substrates or silicon wafers. After the solvent was removed at room temperature, the copolymer film was annealed at 160 °C in a vacuum oven for 24 h. Both the heating and cooling rates were controlled at 0.5 °C/min. The microphase separation of the block copolymer films was explored at room temperature with an atomic force microscope (AFM, SII 4000) in tapping mode.

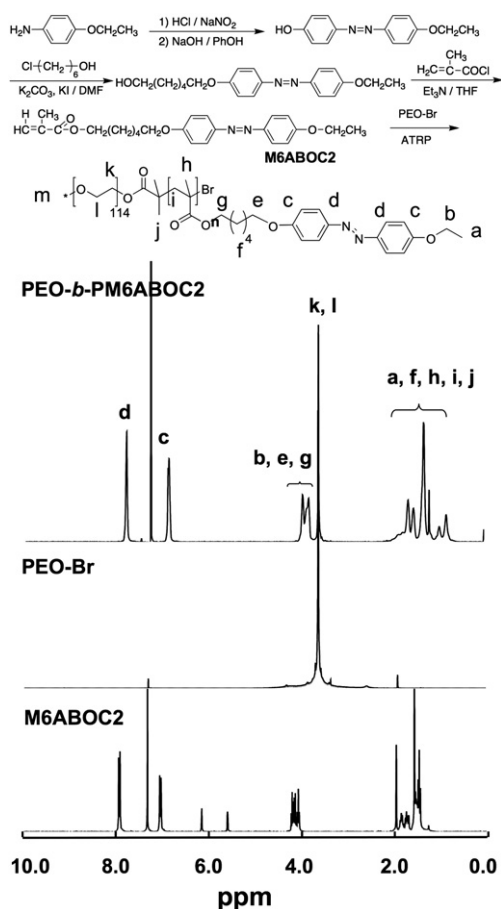


Fig. 1. Synthetic scheme and  $^1\text{H}$  NMR spectra of the monomer M6ABOC2, the macroinitiator PEO-Br and the amphiphilic nematic LCBC.

A linearly polarized laser beam from an  $\text{Ar}^+$  laser (488 nm) at an intensity of  $50 \text{ mW/cm}^2$  was used to induce alignment of AZ mesogens. The transmittance of a He–Ne laser at 633 nm with weak intensity was measured simultaneously during irradiation through a pair of crossed polarizers, with the sample films between them. After the photoalignment, the film was annealed at  $150^\circ\text{C}$  to enhance the alignment. The film anisotropy was characterized with polarized UV–vis absorption spectra and POM images.

### 3. Results and discussion

Fig. 1 shows the synthetic scheme and  $^1\text{H}$  NMR spectra of the monomer M6ABOC2, the macroinitiator PEO-Br and the amphiphilic nematic LCBC. To ensure a nematic LC phase of the designed LCBC, a typical AZ compound M6ABOC2 was used as a mesogenic monomer for a modified atom transfer radical polymerization (ATRP) with a bromo-substituted PEO (PEO-Br) having about 114 repeat units as a macroinitiator [11,12]. The well-specified molecular structure of PEO-*b*-PM6ABOC2 can easily be assigned from its NMR spectra, and about 64 repeat units of the AZ block were estimated by the integration of the phenyl proton NMR peak at 6.82 ppm (proton c in Fig. 1) of the AZ group to that of the oxyethylene protons of the PEO at 3.58 ppm (proton k and l). Referencing against standard polystyrenes with chloroform as eluent, the GPC curve yielded a molecular weight of  $31\,000 \text{ g/mol}$  and a narrow polydispersity index of 1.2, which agrees with the estimated results from NMR analysis, indicating a well-defined molecular structure of the obtained LCBC.

Fig. 2 shows thermal properties of the novel amphiphilic nematic LCBC. In its thermogram by DSC (Fig. 2a), two phase-transition peaks on heating appeared at  $43^\circ\text{C}$  and  $154^\circ\text{C}$ , corresponding to the PEO melting point and the nematic LC to isotropic phase transition, respectively. An obvious glass transition temperature ( $T_g$ ) was observed at  $76^\circ\text{C}$ , which was attributed to the AZ LC block. This thermal property is similar to the homopolymer PM6ABOC2, as reported by Ikeda et al. [23]. On cooling, a clearing point appeared at  $146^\circ\text{C}$  due to the overcooling effect. Interestingly, the PEO melting point was observed at  $-34^\circ\text{C}$ , far lower than that in the heating process, which might be originated from the confined crystallization by microphase separation [24]. A typical Schlieren texture appeared in its POM image at  $120^\circ\text{C}$  (Fig. 2b) upon cooling from the isotropic phase, indicating a nematic LC phase of the obtained LCBC.

In the UV–vis absorption spectrum of the LCBC in chloroform solution (Fig. 3), two peaks appeared at the band of about  $358 \text{ nm}$  and  $455 \text{ nm}$ , owing to the  $\pi-\pi^*$  and  $n-\pi^*$  transitions of AZ chromophores, respectively. For the as-prepared film with a thickness of about  $100 \text{ nm}$  obtained from spin-coating, a blue shift of about  $15 \text{ nm}$  occurred in the maximum absorption peak of the  $\pi-\pi^*$  transition, due to the formation of H-aggregation [25]. However a shoulder peak still remained at  $358 \text{ nm}$ , resulting from the non-aggregated AZs. Then the as-prepared film was annealed at  $160^\circ\text{C}$  for 6 h, and cooled down to room temperature with a speed of  $0.5^\circ\text{C/min}$ . After the annealing, multiple peaks were observed as shown in Fig. 3. The absorbance of the peak at  $343 \text{ nm}$  decreased greatly, which might be attributed to the out-of-plane arrangement of the AZ mesogens in thin films [10–12]. On the other hand, the absorption peak became broader than that of the as-prepared film. It is well-known that J-aggregation induces a red shift in the

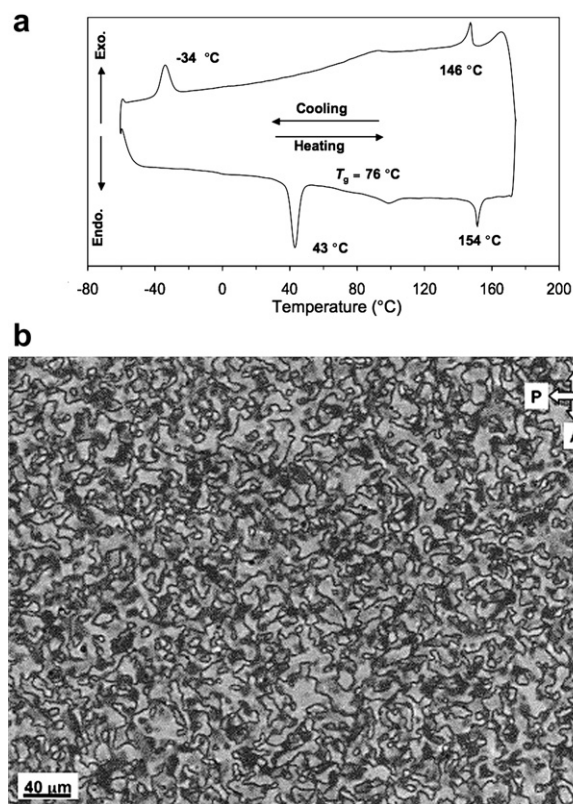


Fig. 2. Thermal properties of PEO-*b*-PM6ABOC2. (a) Heating and cooling DSC curves (the third scan).  $T_g$  is the glass transition temperature. (b) POM image obtained at  $120^\circ\text{C}$ . A: analyzer; P: polarizer.

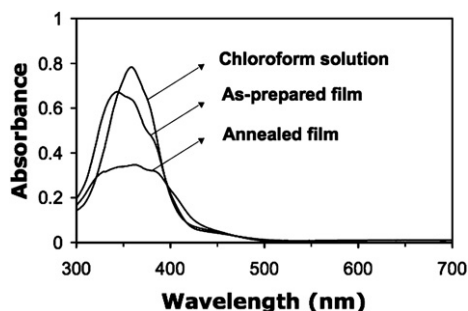


Fig. 3. UV-vis absorption spectra of the LCBC in chloroform, as-prepared and annealed films.

absorption of chromophores [26]. Therefore, H-aggregation, J-aggregation and non-aggregated AZs might simultaneously exist in the annealed film [25–27]. Such aggregation behaviors were different from the thermally-annealed films of smectic LCBCs, where H-aggregation and non-aggregated AZs were involved and no J-aggregation was observed [10–12].

In thin films of smectic LCBCs, previous studies [10–12] carried out vertical alignment of a PEO nanocylinder array with hexagonal packing, which might be attributed to the SMCM of the microphase-separated nanocylinder with the out-of-plane arranged smectic LCs in a 2D order. A similar microphase-separated nanostructure was observed in the AFM images of the present nematic LCBC film, as shown in Fig. 4. In this work, all AFM images are phase images obtained in tapping mode. No nanostructures appeared clearly in the as-prepared film because the microphase separation might be blocked in the glassy state at room temperature. To accelerate the thermodynamically driven process of microphase

separation, the as-prepared film was annealed in a vacuum oven at 160 °C, a little higher than the nematic LC to isotropic phase-transition temperature. After annealing for 2 h, obviously disordered nanostructures with irregular domain sizes were observed (see Fig. 4b), which might be due to the incomplete microphase separation within a short annealing time. It must be mentioned that the dark parts in the images were PEO domains due to the difference in elastic modulus between the hydrophilic PEO block and the hydrophobic AZ mesogenic segment. Both nanodots and nanostripes were found in Fig. 4c, indicating the formation of PEO nanocylinders upon microphase separation after annealing for 4 h. However, the nanocylinders were aligned randomly: some of them were normal to the substrate and others in plane. In Fig. 4d, all the nanostripes were changed into nanodots with a diameter of about 6 nm, demonstrating that all the PEO nanocylinders were aligned normally to the substrate after the annealing for 6 h. The fast Fourier transform (FFT) image in a small area of Fig. 4d showed a distorted hexagon, indicating a well-defined morphology with a modified hexagonal packing of the PEO nanocylinders [14]. No obvious change in the microphase-separated nanostructure was observed with a longer annealing time. Unfortunately, perfectly hexagonal packing of the PEO nanocylinders could not be obtained in the whole area of the nematic LCBC films, which is slightly different from that of the smectic LCBC films [10–12].

Annealing the LCBC films at a temperature in the isotropic phase is one of the key factors to obtain well-defined morphologies of the perpendicular orientation of microphase-separated PEO nanocylinders. The SMCM functioned as the interaction between the self-organization of the LC block and microphase separation of the amphiphilic incomparable diblock copolymers. At an elevated temperature of 160 °C, the amphiphilic nematic LCBC was liquid-like, and both the PEO block and the AZ block had sufficient mobility to self-assemble [28]. However the self-organization of

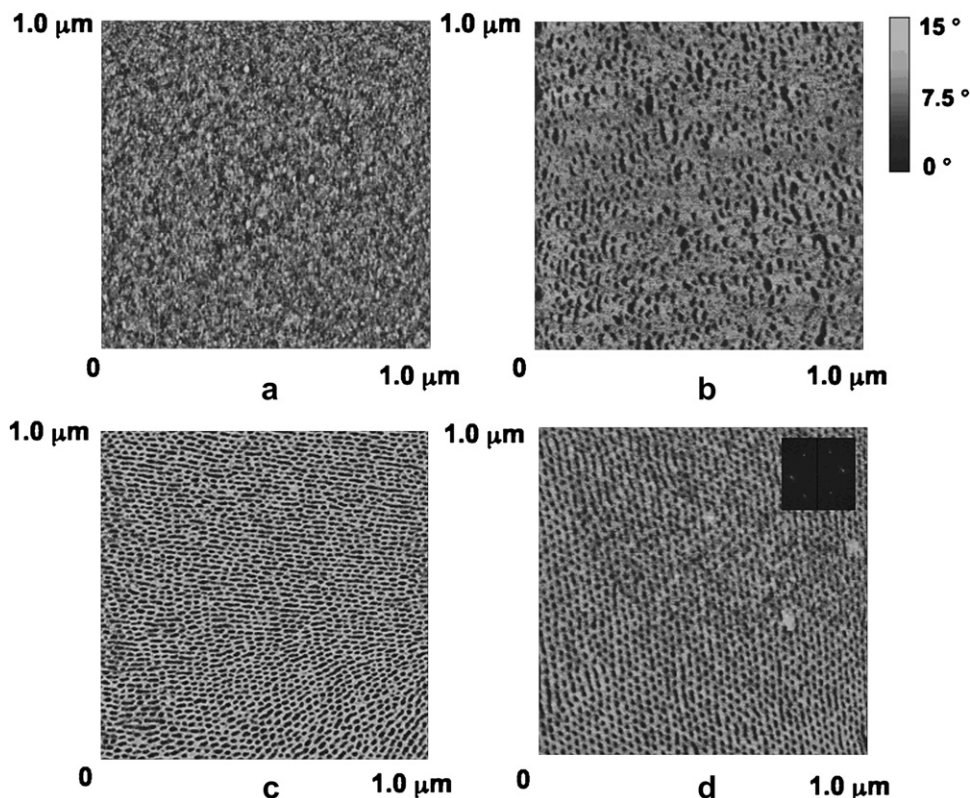


Fig. 4. AFM phase images of the nematic LCBC with different annealing times. (a) 0 h, (b) 2 h, (c) 4 h, (d) 6 h. The inset picture of (d) is the fast Fourier transform of a small area.

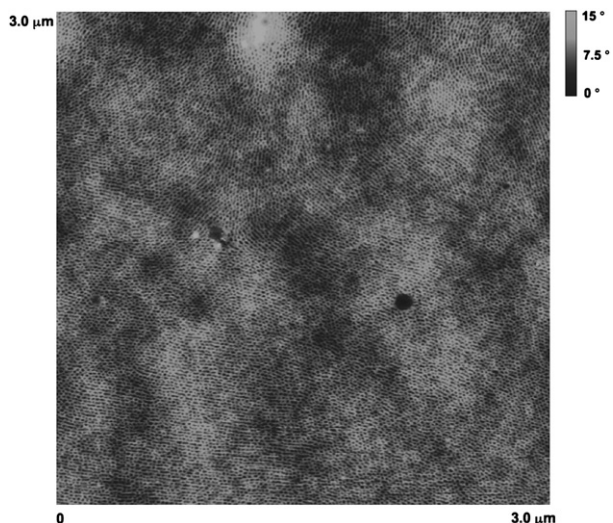


Fig. 5. AFM phase image of PEO-*b*-PM6ABOC2 film after annealing for 6 h with a large area of  $3 \mu\text{m} \times 3 \mu\text{m}$ .

the LCBC could not reach an equilibrium morphology in a short time, which led to a disordered nanostructures in Fig. 4b,c. By gradually decreasing the temperature after the annealing for 6 h, the AZ block first underwent an isotropic to nematic LC phase transition and the AZ block formed the major phase in bulk films due to its large volume ratio. The AZ blocks self-organized in its nematic LC phase in 1D order, which still exerted a force on the liquid-like PEO domains according to the SMCM, resulting in a vertically orientated patterning of nanocylinder arrays in Fig. 4d. Then the microphase separation was frozen when temperature went below  $T_g$  of the AZ block. Finally, the PEO block slowly crystallized among the glassy nematic LC domains, which did not influence the finally obtained microphase separation.

In thin films of the nematic LCBC, the modified hexagonal packing of the PEO nanocylinder array with perpendicular orientation to the substrate can be observed in the whole area of the substrates. For microphase separation in amorphous block copolymer films, electric or magnetic field [29,30], temperature gradient [31], crystallization [32], modified surface of substrates [33], mechanical shearing [34], solvent evaporation [35], roll casting [36] have been explored to obtain long-range orders due to the absence

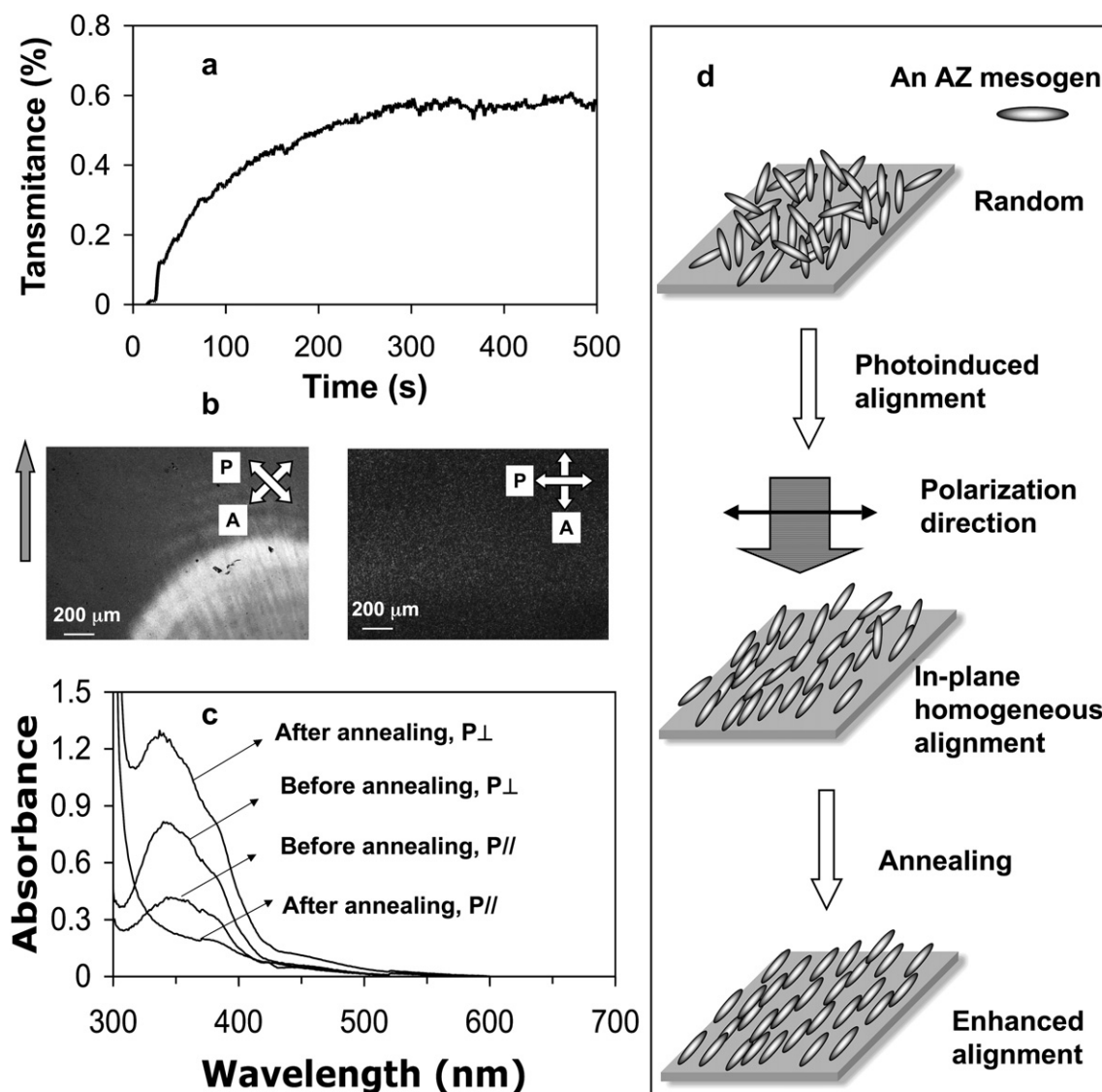


Fig. 6. Photoalignment of the nematic LCBC. (a) Photoinduced change in transmittance with irradiation time. (b) Pictures of the aligned film sandwiched with two crossed polarizers. The arrow is the polarization direction of the linearly polarized beam. (c) Polarized UV–vis absorption spectra of the aligned film before and after annealing.  $P_{\perp}$  and  $P_{\parallel}$  are the absorption curves perpendicular and parallel to the polarization direction of the linearly polarized beam, respectively. (d) Scheme of photoinduced alignment and its enhancement of AZ LC mesogens.

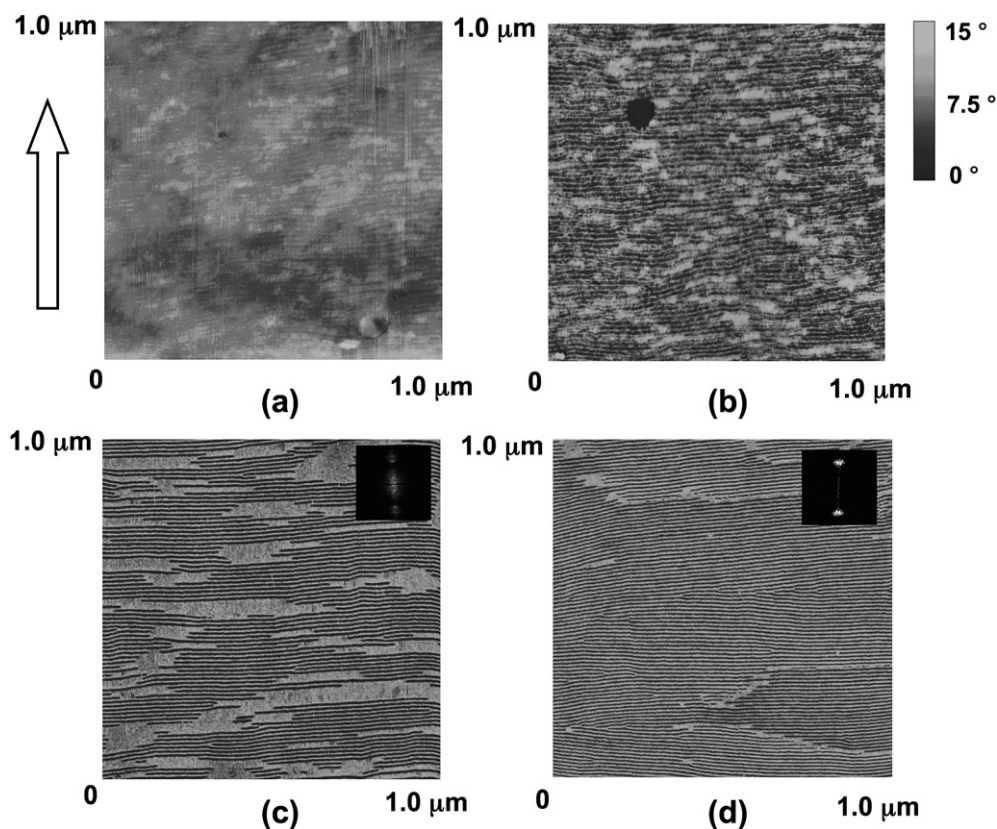


Fig. 7. AFM phase images of photoalignment films of PEO-*b*-PM6ABOC2 with different annealing time. (a) 0 h, (b) 2 h, (c) 4 h, (d) 6 h.

of SMCM. Although no specific external driving forces were exerted on the nematic LCBC films, the vertically patterning of the PEO nanocylinders was obtained in a macroscopic scale, which is similar to the work of Stamm and Laforge [37–39]. Owing to the AFM resolution, a large area of  $3\ \mu\text{m} \times 3\ \mu\text{m}$  is given in Fig. 5. In fact, such dotted patterning of PEO nanocylinders could be easily achieved over several centimeters, which were confirmed by acquiring AFM images spaced by  $100\ \mu\text{m}$  over the whole substrate.

To fabricate parallel patterning of the PEO nanocylinders in plane, the LC block should be homogeneously aligned based on the SMCM [10,11]. This work chose a non-contact method of photoalignment of the nematic AZ mesogens. The reason is that since the viscosity of the nematic AZ mesogens was lower than that of the smectic LCs, they might allow obtaining quick photoresponse. The as-prepared film was irradiated with a linearly polarized beam with a diameter of about 2.0 mm. A He–Ne laser at 633 nm with weak intensity was adopted as a probe beam since there was no absorption at this wavelength in the UV–vis absorption spectrum of the LCBC film (Fig. 2a). Fig. 6a shows the photoinduced change in transmittance ( $T$ ) of the LCBC film, measured simultaneously during the irradiation through two crossed polarizers with the sample films between them. Before the irradiation, no  $T$  was observed because no alignment of the mesogens was induced in film-forming process of spin coating. Upon irradiation, photoalignment of AZs with their transition moments almost perpendicular to the polarization direction of the incident light occurred according to the Weigert effect [40], which led to a quick initial increase in  $T$ . After 300 s,  $T$  gradually increased to a plateau value and no obvious increase was induced with a longer irradiation time, indicating a photostationary state. The photoalignment of LCs can also be confirmed by POM pictures (see Fig. 6b). When the sample film was tilted by  $45^\circ$  with respect to the polarization direction of the laser beam and the polarizer, a bright

circular image with a diameter of about 2.0 mm was clearly observed in the irradiated area. Whereas a dark image appeared when the sample film was tilted by  $0^\circ$  or  $90^\circ$ , such alternating bright and dark sphere images appeared with a periodicity of  $90^\circ$ . No change was observed in  $T$  in the un-irradiated area when rotating the sample film, demonstrating that the photoalignment occurred only in the laser-irradiated area.

After the photoalignment, the nematic LCBC film exhibited intensive anisotropy in its polarized UV–vis spectra as shown in Fig. 6c, which indicates that the homogeneous LC alignment was

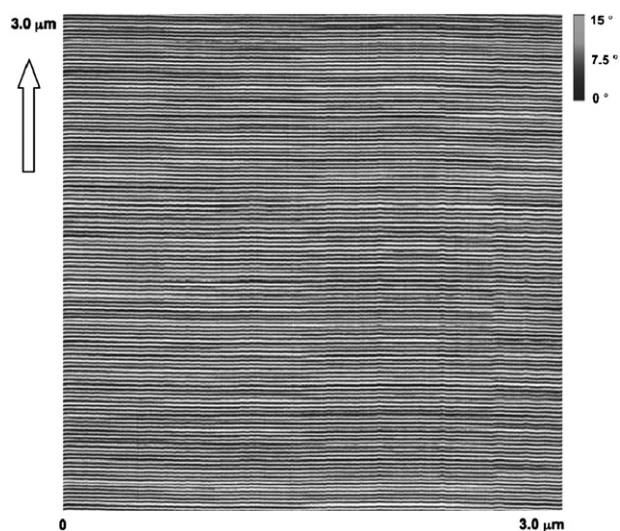


Fig. 8. AFM phase image of photoalignment films PEO-*b*-PM6ABOC2 after annealing for 6 h with a large area of  $3\ \mu\text{m} \times 3\ \mu\text{m}$ .

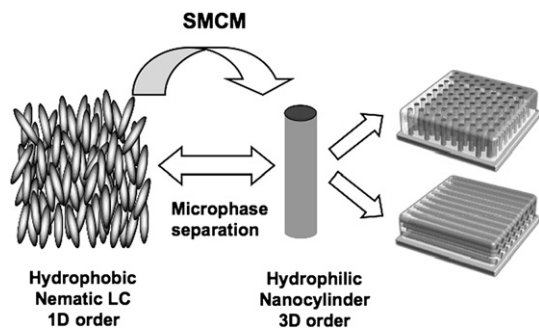


Fig. 9. Possible mechanism of the SMCM in the present LCBC with a nematic phase.

achieved perpendicular to the polarization of the actinic light. The order parameter ( $S$ ) of 0.22 at 343 nm was calculated by  $S = (A_{\infty} - A_{//}) / (A_{\infty} + 2A_{//})$ , where  $A_{\infty}$  and  $A_{//}$  are the absorbance perpendicular and that parallel to the polarization direction of the laser beam, respectively [22]. No homogeneous alignment of LCs occurred in the un-irradiated area because  $S = 0$  was obtained. After being annealed at 150 °C for 6 h,  $S = 0.58$  was calculated in the irradiated area of the film, indicating the enhanced alignment of ordered mesogens upon annealing. Fig. 6d depicts a possible scheme of photoalignment and its enhancement of nematic LC mesogens upon annealing. The chosen annealing temperature of 150 °C was just slightly lower than the nematic LC to isotropic phase transition, which is very important for preparing the parallel patterning of the nanostructures [41]. Firstly, the viscosity of the film is decreased and the molecular mobility is improved at the elevated temperature, which leads to the enhancement of the LC ordering pre-aligned by the actinic laser beam owing to the molecular cooperative motion, one of the inherent properties of LCs [2]. Secondly, the microphase separation might proceed quickly in the less viscous film. Thirdly, the nematic phase have a strong influence on the SMCM of the LCBC, transferring the LC ordering to the microphase-separated nanostructures.

Fig. 7 shows the microphase-separated nanostructures of the photoalignment films with different annealing times. Without annealing, ambiguous nanostructures were observed in Fig. 7a because of the frozen microphase separation in the LCBC film. After 2 h of annealing, parallel patterning of the PEO nanocylinders with irregularity and many defects could be dimly recognized from Fig. 7b, due to the uncompleted microphase separation within the short annealing time. Although defects still existed in Fig. 7c after 4 h of annealing, almost regularly parallel patterning of the PEO nanocylinders in plane was indicated by the FFT image in the whole area. Then almost homogeneous alignment in plane of the nanocylinders was obtained in Fig. 7d after 6 h of annealing. Being dispersing in the major phase of the AZ nematic LC block, about 86 nanocylinders with a diameter of about 6 nm were detected in an area of 1  $\mu\text{m}^2$ . All the nanocylinders penetrated the whole area in Fig. 7d, showing a length of about 1000 nm, and a periodicity of about 12 nm. The alignment of the PEO nanocylinders was parallel to the AZ mesogens and perpendicular to the polarization direction of the actinic laser beam, implying that the SMCM worked well in the present nematic LCBC although it only showed 1D order.

Recently, photocontrolled parallel patterning of nanostructures was obtained in a polystyrene (PS)-based smectic LCBC [16]. Although the microphase separation followed the working principle of the SMCM, defects was found because of the high  $T_g$  of the PS block, which led to uncompleted microphase separation. Very luckily, almost perfect homogeneous alignment of PEO nanocylinder arrays was achieved because of the low crystallized temperature of the flexible PEO block (about -30 °C due to confinement of microphase separation, as shown in Fig. 2a) [11,24].

Similar results were obtained in the photoalignment film of the present nematic LCBC. Following the SMCM, although only 1D order from the continuous phase of the nematic LC block was converted to the PEO nanocylinders, its parallel patterning in plane exhibited a macroscopic order, as shown in Fig. 8. About 260 nanocylinders with a length of 3  $\mu\text{m}$  were homogeneously patterned in an area of 3  $\mu\text{m} \times 3 \mu\text{m}$ . In fact, such a regularity of nanocylinders patterning in plane could be extended to the whole irradiated area (a circle with a diameter of about 2 mm).

The possible functions of SMCM in the nematic LCBC film can be schematically illustrated in Fig. 9, in which both the LC alignment and microphase-separated nanostructures are described. The thermal annealing in an isotropic phase can induce vertical alignment of nanostructures, whereas photoalignment with a linearly polarized light causes in plane alignment of nanocylinders. Although the major phase of the hydrophobic nematic LC block shows only 1D order, it can endow the minor phase of the hydrophilic PEO nanocylinders with 3D order. Both homeotropic and homogenous patterns of the microphase-separated nanocylinders were successively fabricated, coinciding with the alignment direction of the nematic LC block.

#### 4. Conclusions

In summary, an amphiphilic LCBC with an azobenzene moiety as a nematic mesogen was prepared by a modified atom transfer radical polymerization. Upon microphase separation, the LC block formed the major phase in the well-defined LCBC. Both thermal annealing and photoalignment were used to control the alignment of AZ mesogens in films. Although the LC block showed only 1D ordering, it could endow the minor phase of the hydrophilic PEO nanocylinders with 3D order under the action of SMCM. Because of the fact that the viscosity of the nematic LCBC was lower than that of the smectic one, both homeotropic and homogenous patterns of the microphase-separated nanocylinders were successfully obtained within a short annealing time. Such macroscopically ordered nanostructures in films provide a convenient and low-cost method to fabricate ordered patterning of nanosize domains smaller than 100 nm by top-down nanotechnology. The microphase-separated nanostructures with high regularity in the obtained nematic LCBC showed excellent reproducibility and mass-production capability, which might guarantee nanotemplated fabrication processes [42–44], and lead to novel industrial applications in macromolecular engineering.

#### References

- [1] Gray GW. In: Demus D, Goodby J, Gray GW, Spiess HW, Vill V, editors. Handbook of Liquid Crystals. Fundamentals, vol. 1. Weinheim: Wiley-VCH; 1998 [chapter 1].
- [2] Ikeda TJ. Mater Chem 2003;13:2037.
- [3] Mao G, Ober CK. Acta Polym 1996;48:405.
- [4] Lee M, Cho BK, Zin WC. Chem Rev 2001;101:3869.
- [5] Walther M, Finkelmann G. Prog Polym Sci 1996;21:951.
- [6] Yu HF, Kobayashi T. Molecules 2010;15:570.
- [7] Zhao Y, Tong X, Zhao Y. Macromol Rapid Commun 2010;31:986.
- [8] Zhao Y, He J. Soft Matter 2009;5:2686.
- [9] Tian Y, Watanabe K, Kong X, Abe J, Iyoda T. Macromolecules 2002;35:3739.
- [10] Yu HF, Li J, Ikeda T, Iyoda T. Adv Mater 2006;18:2213.
- [11] Yu HF, Iyoda T, Ikeda TJ. Am Chem Soc 2006;128:11010.
- [12] Yu HF, Kobayashi T. ACS Appl Mater Interfaces 2009;1(12):2755.
- [13] Watanabe K, Watanabe R, Aoki D, Shoda S, Komura M, Kamata K, et al. Trans Mater Res Soc Jpn 2006;31:237.
- [14] Komura M, Iyoda T. Macromolecules 2007;40:4106.
- [15] Chen D, Liu H, Kobayashi T, Yu HF. Macromol Mater Eng 2010;295:26.
- [16] Morikawa Y, Takeshi K, Nagano S, Seki T. Chem Mater 2007;19:1540.
- [17] Gohy J, Fustin C, Schumers J. Macromol Rapid Commun 2010;31:1588.
- [18] Okano K, Tsutsumi O, Shishido A, Ikeda TJ. Am Chem Soc 2006;128:15368.
- [19] Zhao Y. Pure Appl Chem 2004;76:1499.
- [20] Yager K, Barrett CJ. Photochem Photobio A Chem 2006;182:250.

- [21] Yu HF, Kobayasi T, Ge Z. *Macromol Rapid Commun* 2009;30:1725.
- [22] Yu HF, Asaoka S, Shishido A, Iyoda T, Ikeda T. *Small* 2007;3:768.
- [23] Ikeda T, Yoneyama S, Yamamoto T, Hasegawa M. *Mol Cryst Liq Cryst* 2003;401(35):149.
- [24] Yu HF, Shishido A, Ikeda T, Iyoda T. *Macromol Rapid Commun* 2005;26:1594.
- [25] Chen D, Liu H, Kobayasi T, Yu HF. *J Mater Chem* 2010;20:3610.
- [26] Menzel H, Weichart B, Schmidt A, Paul S, Knoll W, Stumpe J, et al. *Langmuir* 1926;1994:10.
- [27] Tong X, Cui L, Zhao Y. *Macromolecules* 2004;37:3101.
- [28] Ding L, Mao H, Xu J, He J, Ding X, Russell T, et al. *Macromolecules* 1897;2008:41.
- [29] Morkved T, Lu M, Urbas A, Ehrichs E, Jaeger H, Mansky P, et al. *Science* 1996;273:931.
- [30] Osuji C, Ferreira P, Mao G, Ober C, Vander Sande J, Thomas E. *Macromolecules* 2004;37:9903.
- [31] Bodycomb J, Funaki Y, Kimishima K, Hashimoto T. *Macromolecules* 1999;32:2075.
- [32] Rosa C, Park C, Thomas E, Lotz B. *Nature* 2000;405:433.
- [33] Shin K, Xiang H, Moon S, Kim T, McCarthy T, Russell T. *Science* 2004;306:76.
- [34] Angelescu D, Waller J, Register R, Chikin P. *Adv Mater* 2005;17:1878.
- [35] Kim S, Misner M, Xu T, Kimura M, Russell T. *Adv Mater* 2004;16:226.
- [36] Honeker C, Thomas E, Albalak R, Hajduk D, Gruner S, Capel M. *Macromolecules* 2000;33:9395.
- [37] Sidorenko A, Tokarev I, Minko S, Stamm M. *J Am Chem Soc* 2003;125:12211.
- [38] Tokarev I, Krenek R, Burkov Y, Schmeisser D, Sidorenko A, Minko S, et al. *Macromolecules* 2005;38:507.
- [39] Laforgue A, Bazuin CG, Prud'homme RE. *Macromolecules* 2006;39:6473.
- [40] Weigert F. *Verh Dtsch Phys Ges* 1919;21:485.
- [41] Han D, Tong X, Zhao Y, Zhao Y. *Angew Chem Int Ed* 2010;49:9162.
- [42] Li J, Kamata K, Watanabe S, Iyoda T. *Adv Mater* 2007;19:1267.
- [43] Watanabe S, Fujiwara R, Hada M, Okazaki Y, Iyoda T. *Angew Chem Int Ed* 2007;46:1120.
- [44] Nakamura Y, Murayama A, Watanabe R, Iyoda T, Ichikawa M. *Nanotechnology* 2010;21:095305.